# AOT Reversed Micelles Investigated by Fluorescence Anisotropy of Cresyl Violet†

**Nadine Wittouck,‡ R. Martín Negri,‡ Marcel Ameloot,§ and Frans C. De Schryver*,‡**

*Contribution from the Department of Chemistry, Katholieke Universiteit Leuven, Celestijnenlaan 200F, B-3001 Heverlee, Belgium, and Limburgs Universitair Centrum, Universitaire Campus, B-3590 Diepenbeek, Belgium*

*Received January 24, 1994*⊗

**Abstract:** AOT reversed micelles in *n*-heptane and *n*-dodecane as the continuous phase at various values of $W = [H_2O]/[AOT]$ were investigated through the decay of the total fluorescence, $f(t)$, and of the fluorescence anisotropy, $r(t)$, of cresyl violet. The total fluorescence decay was monoexponential in all cases investigated. The fluorescence lifetime decreased with increasing $W$, with the extent of decrease diminishing at higher $W$ values. No significant dependence on the continuous phase was observed. A biexponential expression for the fluorescence anisotropy yielded adequate fits for all cases. For $W < 10$, one correlation time reflects the internal rotation of the probe in the micelle and the second the overall rotation of the micelle. For $W \geq 10$, the fluorescence anisotropy can be expressed alternatively by $r(t) = r_p(t)\, r_b(t) \exp(-t/\phi_{sph})$; $r_p(t)$ denotes the anisotropy of the dye within its local hindering environment, $r_b(t)$ accounts for the motion of the micellar segment containing the dye, and $\exp(-t/\phi_{sph})$ is the additional depolarization factor associated with the overall rotation of the micelle. Both $r_p(t)$ and $r_b(t)$ were expressed as the sum of an exponential decay and a constant. The constant in the expression of $r_p(t)$ gives an indication of the width of the distribution of the dye within the micellar segment; i.e., the constant is correlated with the second orientational order parameter, $S_p$. Similarly, the constant in the expression for $r_b(t)$ measures the second-order parameter, $S_b$, of the equilibrium distribution of the micellar segments with respect to the normal to the micellar surface. It was found that $S_p$ was about 0.9. The value of $S_p$ did not depend on the continuous phase. In contrast, $S_b$ was higher in *n*-dodecane (0.7) than in *n*-heptane (0.4). The relaxation time, $\phi_b$, in $r_b(t)$ measures the dynamics of the wobbling motion of the micellar segment and was found to be on the order of several nanoseconds. As expected, $\phi_b$ is higher in *n*-dodecane than in *n*-heptane. The motion of micellar segments has been suggested in the literature, and we refer to it as micellar "breathing".

## Introduction

Reversed micelles have received considerable attention in the last few years,[1−5] mainly because of the possibility of performing chemical reactions essentially in an organic phase, but hosting the reactive species in the water pool, e.g., enzymatic reactions,[6] photoelectron transfer reactions,[7−9] proton transfer,[10] singlet oxygen photosensitization,[11] or inverse microemulsion polymerization.[12,13] The aim of the present work is to study AOT reversed micelles at different values of the parameter $W$ = [water]/[AOT] using *n*-heptane and *n*-dodecane as the organic phase. This study is performed by monitoring the fluorescence behavior of the embedded dye cresyl violet (CV). Cresyl violet has been used in several photophysical studies because of its high fluorescence quantum yield in the long-wavelength range of the visible spectrum[14,15] and its high thermal and photochemical stability.[16] CV is also used as a fluorescence standard[17] and as a laser dye.[18] Different applications in spectral and nonphotochemical hole burning,[19,20] as photosensitizer in electron transfer reactions,[21] and in photodynamic therapy[22] have been reported for CV in recent years. The spectroscopic properties in solution were discussed in detail.[23,24] The maximum of the $S_0 \rightarrow S_1$ absorption band of CV in water and alcohols is around 580−595 nm, which is an ideal value for excitation with the normal output of a rhodamine 6G (590 nm) laser dye. This, and the relatively high value of the fluorescence

* To whom correspondence should be addressed.

† Abbreviations: CV, cresyl violet; AOT, bis(2-ethylhexyl) sulfosuccinate sodium salt.

‡ Katholieke Universiteit Leuven.

§ Limburgs Universitair Centrum.

⊗ Abstract published in *Advance ACS Abstracts,* October 15, 1994.

(1) Gelade, E.; De Schryver, F. C. In *Reverse Micelles*; Luisi, P. L., Straub, B. E., Eds.; Plenum Press: New York, 1984; p 143.
(2) Jain, T. K.; Varshney, M.; Maitra, A. *J. Phys. Chem.* **1989**, *93*, 7409.
(3) Lossia, S. A.; Flore, S. G.; Nimmala, S.; Li, H.; Schlick, S. *J. Phys. Chem.* **1992**, *96*, 6071.
(4) Zhang, J.; Bright, F. V. *J. Phys. Chem.* **1992**, *96*, 5633.
(5) Eicke, H.-F.; Gauthier, M.; Hilfiker, R.; Struis, R. P. W.; Xu, G. *J. Phys. Chem.* **1992**, *96*, 5175.
(6) Grandi, C.; Smith, R. E.; Luisi, P. L. *J. Biol. Chem.* **1981**, *256*, 837.
(7) Wong, M; Gratzel, M.; Thomas, J. K. *Chem. Phys. Lett.* **1975**, *30*, 326.
(8) Pileni, M. P. *Chem. Phys. Lett.* **1981**, *81*, 603.
(9) Gauduel, Y.; Migus, A.; Martin, J. L.; Antonetti, A. *Chem. Phys. Lett.* **1984**, *108*, 319.
(10) Bardez, E.; Gouguillon, B.; Keh, E.; Valeur, B. *J. Phys. Chem.* **1984**, *88*, 1909.
(11) Redmond, R. *Photochem. Photobiol.* **1991**, *54*, 457.
(12) Voortmans, G.; De Schryver, F. C. In *Structure and Reactivity in Inverted Micelles*; Pileni, M. P., Ed.; Studies in Physical and Theoretical Chemistry, No. 61; Elsevier: Amsterdam, 1989; p 221.
(13) Candau, F.; Zekhnini, Z.; Durand, J. P. *J. Colloid Interface Sci.* **1986**, *114*, 398.
(14) Magde, D.; Brannon, J. H.; Olmsted, J., III. *J. Phys. Chem.* **1979**, *83*, 696.
(15) Sens, R.; Drexhage, K. H. *J. Lumin.* **1981**, *24/25*, 709.
(16) Olmsted, J., III. *J. Phys. Chem.* **1979**, *83*, 2581.
(17) Eaton, D. F. *Pure Appl. Chem.* **1988**, *60*, 1107.
(18) Drexhage, K. H. In *Dye Lasers;* Schafer, E. P., Ed.; Springer-Verlag: New York, 1977; Chapter 4.
(19) Renn, A.; Bucher, S. E.; Meixner, A. J.; Meister, E. C.; Wild, V. P. *J. Lumin.* **1988**, *39*, 181.
(20) Shu, L. C.; Small, G. J. *J. Opt. Soc. Am. B* **1992**, *9*, 724.
(21) Kreller, D. I.; Kamat, P. V. *J. Phys. Chem.* **1991**, *95*, 4406.
(22) Cincotta, L.; Foley J. W.; Cincotta, A. H. *Photochem. Photobiol.* **1987**, *46*, 75.
(23) Isak, S. J.; Eyring, E. M. *J. Phys. Chem.* **1992**, *96*, 1738.
(24) Isak, S. J.; Eyring, E. M. *J. Photochem. Photobiol., A* **1992**, *64*, 343.

0002-7863/94/1516-10601$04.50/0 

quantum yield, $\Phi_f$, allows a fast collection of the fluorescence decays under normal experimental conditions. The rotational dynamics of CV in homogeneous media have been reported in several studies.[25-37] The rotational motion of CV is sensitive to the local solvation[28] so that the microenvironment of the probe can be monitored by its influence on the rotational motion of the dye. However, this feature has not been used to study the properties of microheterogeneous systems such as micelles and lipid vesicles.

With respect to the studies in AOT/water/*n*-alkane reversed micelles, cresyl violet perchlorate shows two important characteristics: (i) it is soluble in water but is not soluble in *n*-alkanes like *n*-heptane or *n*-dodecane; (ii) it is positively charged while the AOT polar head is negatively charged. Therefore, CV can be expected to be located in the water core of the micelle but near the surfactant molecules. Consequently, the rotational behavior of the probe CV is expected to give information about the dynamics of the surfactant molecules in the micelle. In this paper the rotational motion of the dye is inferred from steady-state and time-resolved fluorescence anisotropy measurements.

## Materials and Methods

**Materials and Sample Preparation.** Cresyl violet perchlorate (Aldrich, laser dye grade) and nile blue hydrochloride (Aldrich) were used as provided. AOT (bis(2-ethylhexyl) sulfosuccinate sodium salt, Fluka) was purified as usual.[3,5] The purified product was dried for 48 h at reduced pressure at 35 °C, and stored under vacuum. This procedure was repeated each time before preparing samples. *n*-Heptane (Merck, Uvasol) was distilled over sodium to reduce the water content in the solvent. *n*-Dodecane (Aldrich, stored under nitrogen atmosphere) was used as provided. Water was purified by a Millipore Super-Q system (pH 7.4).

In the experiments with AOT, a fresh aqueous CV stock solution (pH 7.4) was prepared. The dye concentration in that stock solution in different experiments ranged between $3 \times 10^{-6}$ and $5 \times 10^{-5}$ M. Typically a dye concentration of $5 \times 10^{-6}$ M was used. To obtain a defined $W$ value, the necessary microliters from the stock solution were injected in 4 mL of organic solvent solution (*n*-heptane or *n*-dodecane) containing AOT. The calculation of $W$ was done assuming that the value of $W$ in the dry surfactant is approximately 0.7.[2] Surfactant concentrations were 0.05 and 0.10 M in *n*-heptane and 0.10 M in dodecane. At these [surfactant]/[dye] ratios, and considering the aggregation number of AOT reversed micelles,[38] the average number of probe molecules per micelle is at most one. The solutions were shaken and then stirred at room temperature for 5 min. No turbidity was observed. All experiments were performed with freshly nondegassed solutions at 20 ± 1 °C. In *n*-heptane the range of $W$ values was between 2 and 40. In *n*-dodecane it was only possible to solubilize water up to $W = 20$. Solutions of cresyl violet perchlorate in water (decay time $\tau = 2.02 \pm 0.02$ ns) or nile blue in methanol ($\tau = 1.3 \pm 0.1$ ns)[39] were used as references in the deconvolution of the decays.

**Instrumentation.** The absorption measurements were performed at 20 ± 1 °C with a Perkin-Elmer Lambda 6 UV−vis spectrophotometer.

Steady-state fluorescence excitation spectra were obtained with a SPEX spectrofluorometer. The corrected fluorescence emission spectra were recorded using an SLM-8000C spectrofluorometer.

Stationary fluorescence anisotropy measurements were carried out with an SLM-8000C spectrofluorometer in L-format, correcting for polarization bias in the detection system. The temperature, monitored inside the cuvette (quartz, 1 cm) using a RPt100 resistor, was controlled (±0.5 °C) by a Lauda RUL 480 thermostat−cryostat.

The emission decays were obtained by the single-photon timing technique. The samples were excited by the output of a cavity-dumped, rhodamine 6G dye laser (590 nm), synchronously pumped by a mode-locked argon ion laser. The details of the equipment are given elsewhere.[40,41] Each polarized intensity decay had about $10^4$ counts in the peak channel. The total number of channels was 511. Time increments of 18, 23, and 34 ps per channel were used.

**Equations and Data Analysis.** The samples are excited with vertically polarized laser pulses. The polarized fluorescence decay curves are collected by setting the axis of the emission polarizer at an angle $\theta$ with respect to the polarization of the electric field of excitation. Emission decays are measured with the emission polarizer axis set at $\theta = 0°$, 90°, and 54.7°. The time-dependent anisotropy decay, $r(t)$, is defined as

$$r(t) = \frac{i_{\parallel}(t) - i_{\perp}(t)}{i_{\parallel}(t) + 2i_{\perp}(t)} \tag{1}$$

where $i_{\parallel}(t)$ and $i_{\perp}(t)$ denote, respectively, the polarized fluorescence decays with the emission polarizer set parallel ($\theta = 0°$) and perpendicular ($\theta = 90°$) to the polarization direction of the excitation light. The time-dependent polarized intensities can be written as

$$i_{\parallel}(t) = (1/3)f(t)[1 + 2r(t)] \tag{2}$$

$$i_{\perp}(t) = (1/3)f(t)[1 - r(t)] \tag{3}$$

with $f(t)$ the decay of the total fluorescence, which can be measured with the emission polarizer set at the "magic angle", $\theta = 54.7°$.

In general $r(t)$ is given by

$$r(t) = \sum_{k=1}^{m} \beta_k \exp(-t/\phi_k) \tag{4}$$

where $\phi_k$ ($1 \le k \le m$) denotes the rotational correlation time. The sum of the anisotropy preexponential factors, $\beta_k$, is the initial anisotropy, also called fundamental anisotropy, $r_0$,

$$\sum_{k=1}^{m} \beta_k = r_0 \tag{5}$$

The fundamental anisotropy $r_0$ is a characteristic of the fluorophore and depends on the angle between the absorption

(25) Blanchard, G. J.; Wirth, M. J. *J. Chem. Phys.* **1985**, *82*, 39.
(26) Dutt, G. B.; Doraiswamy, S.; Periasamy, N.; Venkataraman, B. *J. Chem. Phys.* **1990**, *93*, 8498.
(27) Dutt, G. B.; Doraiswamy, S. *J. Chem. Phys.* **1992**, *96*, 2475.
(28) Blanchard, G. J. *J. Chem. Phys.* **1987**, *87*, 6803.
(29) Blanchard, G. J.; Wirth, M. J. *J. Phys. Chem.* **1986**, *90*, 2521.
(30) Blanchard, G. J. *Anal. Chem.* **1989**, *61*, 2394.
(31) Von Jena, A.; Lessing, H. E. *Chem. Phys.* **1979**, *40*, 245.
(32) Millar, D. P.; Shah, R.; Zewail, A. H. *Chem. Phys. Lett.* **1979**, *66*, 435.
(33) Gudgin-Templeton, E. F.; Kenney-Wallace, G. A. *J. Phys. Chem.* **1986**, *90*, 2896.
(34) Beddard, G. S.; Doust, T.; Porter, G. *Chem. Phys.* **1981**, *61*, 17.
(35) Alavi, D. S.; Hartman, R. S.; Waldeck, D. H. *J. Chem. Phys.* **1990**, *92*, 4055.
(36) Baran, J.; Langley, A. J.; Jones, W. *J. Chem. Phys.* **1984**, *87*, 305.
(37) Waldeck, D.; Cross, Jr., A.; McDonald, D.; Fleming, G. R. *J. Chem. Phys.* **1981**, *74*, 3381.
(38) Maitra, A. *J. Phys. Chem.* **1989**, *93*, 7409.
(39) Mylinski, P.; Wieczorek, D.; Kownacki, K. *Chem. Phys. Lett.* **1989**, *155*, 256.
(40) Khalil, M. M. H.; Boens, N.; Van der Auweraer, M.; Ameloot, M.; Andriessen, R.; Hofkens, J.; De Schryver, F. C. *J. Phys. Chem.* **1991**, *95*, 9375.
(41) Van den Zegel, M.; Boens, N.; Daems, D.; De Schryver, F. C. *Chem. Phys.* **1986**, *101*, 311.

and emission dipole moments. For excitation in the $S_0 \rightarrow S_1$ band the theoretical maximum value of $r_0$ is 0.4, which corresponds to the case of collinear dipole moments.

When $f(t)$ is given by

$$f(t) = \sum_{j=1}^{n} \alpha_j \exp(-t/\tau_j) \tag{6}$$

$i_{\parallel}(t)$ and $i_{\perp}(t)$ can generally be written as[42]

$$i_{\parallel}(t) = (1/3)\sum_{j=1}^{n} \alpha_j \exp(-t/\tau_j)[1 + 2\sum_{k=1}^{m} L_{jk}\beta_k \exp(-t/\phi_k)] \tag{7}$$

$$i_{\perp}(t) = (1/3)\sum_{j=1}^{n} \alpha_j \exp(-t/\tau_j)[1 - \sum_{k=1}^{m} L_{jk}\beta_k \exp(-t/\phi_k)] \tag{8}$$

where the factors $L_{jk}$ are equal to unity if the relaxation time $\tau_j$ is associated with the correlation time $\phi_k$ and zero otherwise.

To maximize the flexibility of the analysis program, the polarized intensity with the emission polarizer set at an angle $\theta$, $i(\theta,t)$, is written as[43]

$$i(\theta,t) = [\kappa(\theta)/3]\sum_{j=1}^{n} \alpha_j \exp(-t/\tau_j)[1 + (3\cos^2\theta - 1) \times \sum_{k=1}^{m} L_{jk}\beta_k \exp(-t/\phi_k)] \tag{9}$$

$\kappa(\theta)$ in eq 9 is a matching factor for $i(\theta,t)$. This factor accounts for the differences in the response of the detection system and in the collection time between the different collected polarized decays $i(\theta,t)$. We have shown that the use of a freely adjustable $\kappa(\theta)$ does not introduce additional difficulties in the parameter recovery.[43] In that approach $\kappa(\theta)$ is treated as an additional fitting parameter (only one $\kappa(\theta)$ is fixed to an arbitrary value during the analysis; e.g., $\kappa(0°) = 1$ = constant). The same approach has been used in the current study.

The polarized unmatched decays collected at different angles $\theta$ (=0°, 54.7°, 90°) were simultaneously analyzed using global analysis.[44] The anisotropy analysis program is part of a global analysis program which has been described earlier.[45] In this method all the parameters common to the polarized decays ($\alpha_j$, $\tau_j$, $\beta_k$, and $\phi_k$) are linked and then simultaneously calculated in a single-step analysis. The parameters $\beta_k$ can be freely adjustable during the analysis, or can be constrained to keep $\Sigma\beta_k = r_0$ = constant. The numerical statistical tests include the calculation of the global reduced $\chi^2$ ($\chi_g^2$) and the corresponding $Z_{\chi_g^2}$ ($Z_{\chi_g^2} = (\nu/2)^{1/2}(\chi_g^2 - 1)$, where $\nu$ represents the number of degrees of freedom for the entire multidimensional fluorescence decay surface). $\delta$ function convolution, using the decay of a monoexponentially decaying reference compound, collected at the magic angle, was used in the deconvolution of the polarized decays.[43,46] The fluorescence lifetime of the reference compound was a freely adjustable parameter in the analyses. All global analyses were performed on an IBM RISC 6150-125 computer.

The results obtained were independent of the reference solution and the time increment per channel. The steady-state anisotropy, $\langle r \rangle$, is given by

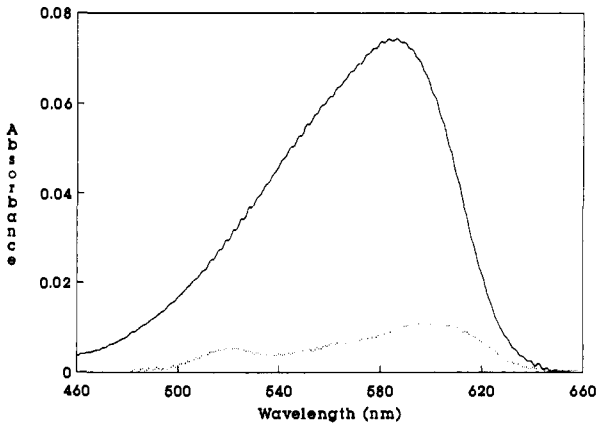


**Figure 1.** 1: Absorption spectra of cresyl violet in pure water and in AOT/water/*n*-heptane reversed micelles: (—): cresyl violet stock in pure water ($3 \times 10^{-6}$ M, pH 7.4); (···) $W = 42$ ([AOT] = 0.10 M).

$$\langle r \rangle = \frac{\int_0^\infty r(t) f(t)\, dt}{\int_0^\infty f(t)\, dt} = \frac{\sum_{j=1}^{n} \alpha_j \gamma_j}{\sum_{j=1}^{n} \alpha_j \tau_j} \tag{10}$$

where

$$\gamma_j = \sum_{k=1}^{m} L_{jk}\beta_k \phi_k \tau_j/(\phi_k + \tau_j) \tag{11}$$

## Results

**Absorption, Emission, and Excitation Spectra. AOT/Water/*n*-Heptane and AOT/Water/*n*-Dodecane.** The maximal absorbances of the solutions investigated are 1−3 orders of magnitude lower than the maximal absorbance of the corresponding stock solution, depending on the ratio $W$ required (see preparation of the samples in Materials and Methods).

In contrast to the spectrum in water, the presence of two absorption bands was observed in AOT reversed micelles with peaks at approximately 521 and 600 nm, respectively (Figure 1). For $\lambda_{exc} > 560$ nm only one emission band is observed, between 600 and 800 nm, with a maximum at 639 nm (Figure 2). The excitation spectrum in AOT reversed micelles observed at 660 nm is reported in Figure 2.

Similar spectral characteristics for solutions of CV in dimethyl sulfoxide (DMSO) and in AOT reversed micelles were observed. Two absorption bands in the visible region appear also in DMSO with maxima at 607 and 489 nm as reported by Gudgin-Templeton and Kenney-Wallace[33] who mentioned that the second band with a maximum around 490 nm could be due to the neutral molecule.

**Decay of the Total Fluorescence.** Total fluorescence decays were measured using 590 nm as the excitation wavelength. Therefore, all the fluorescence lifetimes discussed refer to the longer wavelength absorption band. All decays were collected under magic angle conditions.

In AOT reversed micelles the single curve analysis indicated that the total fluorescence decay was monoexponential. Excellent fits were obtained by global analysis of the decays collected at six different emission wavelengths in the range 630−680 nm and at a given value of $W$ by linking the single relaxation time. This was done for extreme values of $W$ and for both organic phases. No dependence on the concentration of CV or the time increment per channel used was observed. The values of $\tau$ using *n*-heptane and *n*-dodecane as the continuous phase at a given value of $W$ are comparable (Figure 3 and Tables 1 and 3). The

(42) Beechem, J. M.; Brand, L. *Photochem. Photobiol.* **1986**, *44*, 323.
(43) Crutzen, M; Ameloot, M.; Boens, N.; Negri, R. M.; De Schryver, F. C. *J. Phys. Chem.* **1993**, *97*, 8133.
(44) Beechem, J. M.; Ameloot, M.; Brand, L. *Anal. Instrum.* **1985**, *14*, 379.
(45) Boens, N.; Janssens, L. D.; De Schryver, F. C. *Biophys. Chem.* **1989**, *33*, 77.
(46) Boens, N.; Ameloot, M.; Yamazaki, I.; De Schryver, F. C. *Chem. Phys.* **1988**, *121*, 73.

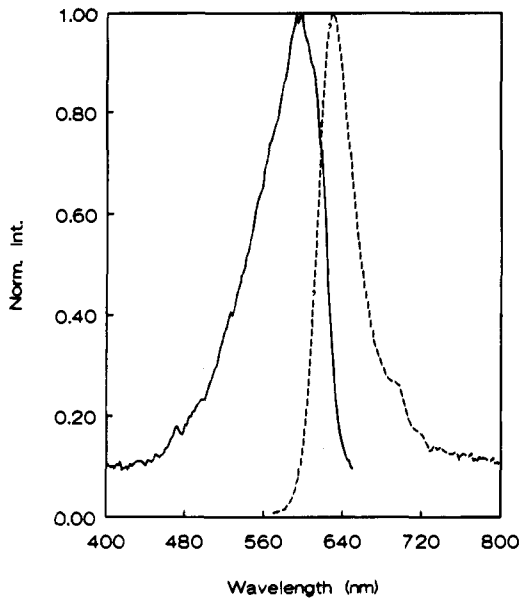


**Figure 2.** 2: Normalized excitation ($\lambda_{em}$ = 660 nm) and emission ($\lambda_{exc}$ = 580 nm) spectra of cresyl violet in AOT/water/*n*-heptane reversed micelles at $W = 42$ ([AOT] = 0.10 M).

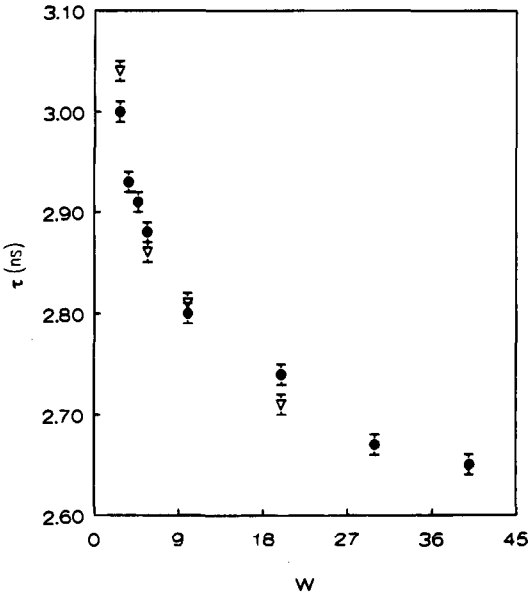


**Figure 3.** 3: Fluorescence lifetime at different values of $W$ ([AOT] = 0.10 M, $\lambda_{exc}$ = 590 nm, and $\lambda_{em}$ is between 620 and 680 nm): (●) *n*-heptane, (▽) *n*-dodecane. The error bars are 1 standard deviation. The numerical values are shown in Tables 1 and 3.

fluorescence lifetime decreases when $W$ increases in *n*-heptane and in *n*-dodecane (Figure 3).

**Fluorescence Anisotropy. (a) Steady-State Anisotropy.** The steady-state fluorescence anisotropy, $\langle r \rangle$, was measured at 19 °C for different values of $W$ for both organic phases at $\lambda_{exc}$ = 580 nm. The reported values of $\langle r \rangle$ (Figure 4) are averages over different emission wavelengths in a range of approximately 30 nm around the maximum of the emission peak to improve the signal to noise ratio. For comparison, $\langle r \rangle$ was also measured in pure water at 19 °C and found to be equal to 0.019 ± 0.005.

At any given value of $W$, the same value of $\langle r \rangle$ was found for [AOT] = 0.05 and 0.1 M in *n*-heptane. In all cases the $\langle r \rangle$ values were higher than in pure water, and decreased from $W = 2$ to $W = 42$ (Figure 4). Values of $\langle r \rangle$ were measured also in AOT/water/*n*-dodecane reversed micelles as a function of $W$ for [AOT] = 0.10 M (Figure 4). A continuous decrease of $\langle r \rangle$ with an increase of $W$ was observed. The values are higher than in AOT/water/*n*-heptane for every value of $W$. Higher

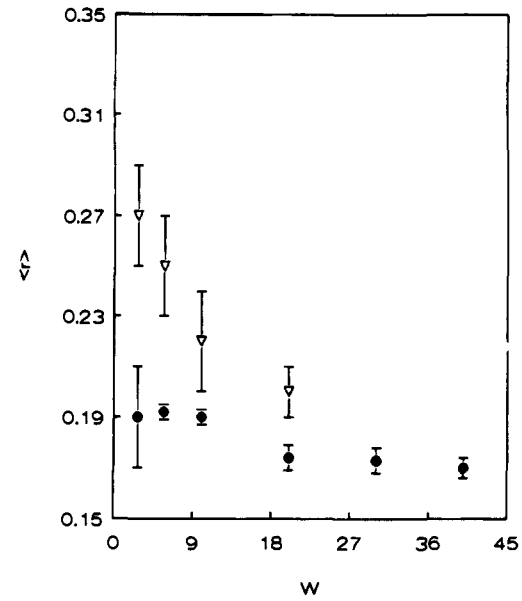


**Figure 4.** 4: Steady-state anisotropy, $\langle r \rangle$ ([AOT] = 0.10 M, $\lambda_{exc}$ = 580 nm, and $\lambda_{em}$ is between 600 and 660 nm): (●) *n*-heptane, (▽) *n*-dodecane. The error bars indicate the standard deviations of the distribution of $\langle r \rangle$ in the considered emission wavelength range.

values of $\langle r \rangle$ for perylene derivatives in AOT/water/*n*-dodecane with respect to AOT/water/*n*-heptane reversed micelles have been reported.[47]

Similar behavior was reported for 1-[4-(trimethylammonio)-phenyl]-6-phenyl-1,3,5-hexatriene (TMA-DPH) tethered at the interface of didodecyldimethylammonium bromide (DDAB) reversed micelles in cyclohexane and alkanes.[48] This could be an indication that the dye is located more near the surfactant polar head than in the water core. However, the steady-state anisotropy is difficult to interpret as its value depends on the fluorescence lifetime (eqs 10 and 11), the possible hindering potential due to the neighboring surfactant molecules, and the rotational motion of the micelle.[49,50] Time-resolved anisotropy experiments might unravel the various contributions and lead to a better picture of the rotational behavior of CV in AOT reversed micelles.

**(b) Time-Resolved Anisotropy.** Time-resolved polarized fluorescence decays of CV in water were measured at different temperatures with $\lambda_{exc}$ = 590 nm and $\lambda_{em}$ = 640 nm. The fluorescence anisotropy, $r(t)$, was well fitted according to model 1:

model 1

$$f(t) = \alpha \exp(-t/\tau) \tag{12a}$$

$$r(t) = \beta \exp(-t/\phi) \tag{12b}$$

This is the most simple model, usually accepted to account for the behavior of CV in alcohols, aprotic solvents, and water.[33,35] According to model 1, the value of $\beta$ should be equal to the fundamental anisotropy $r_0$. In some reports a value of $r_0$ = 0.4 was assumed for CV in alcohols.[28,36,37] Beddard et al.[34] have reported a value of $r_0$ = 0.35 in different solvents. The same value was measured by Alavi et al.[35] in ethanol. To ensure the proper value for CV, we repeated the measurements in propanol (19 °C) using global analysis and duplicated the value

(47) Valeur, B.; Keh, E. *J. Phys. Chem.* **1979**, *83*, 3305.
(48) Chen, V.; Warr, G. G.; Evans, D. F.; Prendergast, F. G. *J. Phys. Chem.* **1988**, *92*, 768.
(49) Szabo, A. *J. Chem. Phys.* **1984**, *81*, 150.
(50) Van der Meer, W.; Pottel, H.; Herreman, W.; Ameloot, M.; Hendrickx, H.; Schroder, H. *Biophys. J.* **1984**, *46*, 515.

**Table 1.** Anisotropy Parameters of Cresyl Violet in AOT/Water/*n*-Heptane Reversed Micelles According to Model 2 (Eq 13)[a]

| $W$ | $\tau$ (ns) | $\phi_{sph}$[b] (ns) | $\phi_1$ (ns) | $\phi_2$ (ns) | $\beta_1$ | $\beta_2$ | $(1/\phi_1 - 1/\phi_{sph})^{-1}$ (ns) | $\chi_g^2$ | $Z_{\chi_g^2}$ |
|---|---|---|---|---|---|---|---|---|---|
| 2.7 | 3.02 ± 0.01 | 3 ± 1 | 1.4[c] | 3.5 ± 0.3 | 0.10 ± 0.02 | 0.28 ± 0.01 | 2.8 ± 1.4 | 1.026 | 0.673 |
| 3.7 | 2.90 ± 0.02 | 5 ± 1 | 1.3 ± 0.5 | 4.4 ± 0.8 | 0.09 ± 0.05 | 0.26 ± 0.05 | 1.8 ± 1.0 | 0.992 | −0.215 |
| 4.7 | 2.90 ± 0.02 | 6 ± 1 | 1.0 ± 0.2 | 4.4 ± 0.5 | 0.09 ± 0.01 | 0.26 ± 0.01 | 1.2 ± 0.3 | 1.045 | 1.151 |
| 5.7 | 2.88 ± 0.02 | 7 ± 1 | 1.4 ± 0.3 | 5.7 ± 0.6 | 0.10 ± 0.02 | 0.25 ± 0.02 | 1.8 ± 0.5 | 0.991 | −0.245 |
| 10 | 2.81 ± 0.01 | 15 ± 2 | 1.8 ± 0.3 | 7 ± 1 | 0.17 ± 0.04 | 0.18 ± 0.04 | 2.0 ± 0.4 | 1.028 | 0.746 |
| 20 | 2.72 ± 0.01 | 40 ± 6 | 1.4 ± 0.2 | 6.6 ± 0.9 | 0.16 ± 0.02 | 0.19 ± 0.02 | 1.5 ± 0.2 | 1.071 | 1.863 |
| 30 | 2.67 ± 0.01 | 111 ± 17 | 1.4 ± 0.1 | 8 ± 2 | 0.20 ± 0.01 | 0.15 ± 0.01 | 1.4 ± 0.1 | 1.092 | 2.458 |
| 40 | 2.64 ± 0.01 | 206 ± 35 | 1.5 ± 0.1 | 10 ± 3 | 0.22 ± 0.02 | 0.13 ± 0.02 | 1.5 ± 0.1 | 1.103 | 2.754 |

[a] [AOT] = 0.10 M; $T$ = 19 ± 1) °C; $W$ = [$H_2O$]/[AOT] and using the constraint $\beta_1 + \beta_2 = 0.35$ except for $W = 2.7$. The fluorescence lifetimes ($\tau$) correspond to the values of Figure 3. The correlation times, $\phi_1$ and $\phi_2$, are represented in Figure 7. [b] Calculated according to eq 21. The indicated uncertainties on $\tau$ and $\phi_k$ ($k$ = 1, 2) are 1 standard deviation. The uncertainties on $\phi_{sph}$ were calculated by assuming a relative error of ±5% for the micellar radius. [c] Fixed during the analysis (see text).

**Table 2.** Anisotropy Parameters of Cresyl Violet in AOT/Water/*n*-Heptane Reversed MIcelles According to Model 2 (Eq 13) with $\phi_2 = \phi_{sph}$ (Table 1)[a]

| $W$ | $\tau$ (ns) | $\beta_1$ | $\beta_2$ | $\phi_1$ (ns) | $S_p$ | $\theta_p$ (deg) | $(1/\phi_1 - 1/\phi_{sph})^{-1}$ (ns) | $\chi_g^2$ | $Z_{\chi_g^2}$ |
|---|---|---|---|---|---|---|---|---|---|
| 2.7 | 3.025 ± 0.006 | 0.052 ± 0.008 | 0.314 ± 0.008 | 1.4[b] | 0.95 ± 0.01 | 15 ± 2 | 2.6 ± 1.0 | 1.028 | 0.731 |
| 3.7 | 2.88 ± 0.02 | 0.10 ± 0.01 | 0.25 ± 0.01 | 1.4 ± 0.2 | 0.85 ± 0.02 | 26 ± 2 | 1.9 ± 0.4 | 1.023 | 0.584 |
| 4.7 | 2.89 ± 0.02 | 0.140 ± 0.006 | 0.210 ± 0.006 | 1.45 ± 0.06 | 0.77 ± 0.01 | 33 ± 1 | 1.9 ± 0.3 | 1.050 | 1.274 |
| 5.7 | 2.876 ± 0.006 | 0.147 ± 0.005 | 0.203 ± 0.005 | 1.83 ± 0.07 | 0.76 ± 0.01 | 34 ± 1 | 2.5 ± 0.2 | 0.991 | −0.230 |
| 10 | 2.807 ± 0.006 | 0.253 ± 0.003 | 0.10 ± 0.003 | 2.49 ± 0.07 | 0.535 ± 0.008 | 50 ± 1 | 3.0 ± 0.1 | 1.030 | 0.782 |
| 20 | 2.723 ± 0.006 | 0.269 ± 0.002 | 0.081 ± 0.002 | 2.35 ± 0.06 | 0.481 ± 0.006 | 53.1 ± 0.4 | 2.50 ± 0.07 | 1.081 | 2.137 |
| 30 | 2.673 ± 0.006 | 0.275 ± 0.002 | 0.075 ± 0.002 | 2.01 ± 0.04 | 0.463 ± 0.006 | 54.2 ± 0.4 | 2.05 ± 0.04 | 1.110 | 2.939 |
| 40 | 2.646 ± 0.006 | 0.279 ± 0.002 | 0.071 ± 0.002 | 1.97 ± 0.04 | 0.450 ± 0.006 | 55.0 ± 0,3 | 1.99 ± 0.04 | 1.112 | 3.007 |

[a] [AOT] = 0.10 M; $T$ = 19 ± 1 °C; $W$ = [$H_2O$]/[AOT] and using the constraint $\beta_1 + \beta_2 = 0.35$ except for $W = 2.7$. [b] Fixed during the analysis.

**Table 3.** Anisotropy Parameters of Cresyl Violet in AOT/Water/*n*-Dodecane Reversed Micelles According to Model 2 (Eq 13)[a]

| $W$ | $\tau$ (ns) | $\phi_{sph}$[b] (ns) | $\phi_1$ (ns) | $\phi_2$ (ns) | $\beta_1$ | $\beta_2$ | $(1/\phi_1 - 1/\phi_{sph})^{-1}$ (ns) | $\chi_g^2$ | $Z_{\chi_g^2}$ |
|---|---|---|---|---|---|---|---|---|---|
| 2.7 | 3.05 ± 0.01 | 12 ± 2 | 2.1 ± 0.9 | 17 ± 2 | 0.05 ± 0.02 | 0.30 ± 0.02 | 2.5 ± 1.3 | 0.970 | −0.654 |
| 5.7 | 2.86 ± 0.01 | 26 ± 4 | 1.8 ± 0.4 | 23 ± 3 | 0.09 ± 0.01 | 0.26 ± 0.01 | 1.9 ± 0.5 | 1.119 | 2.561 |
| 10 | 2.78 ± 0.01 | 52 ± 8 | 1.7 ± 0.2 | 22 ± 2 | 0.11 ± 0.01 | 0.24 ± 0.01 | 1.8 ± 0.2 | 1.108 | 2.398 |
| 20 | 2.71 ± 0.01 | 139 ± 21 | 2.0 ± 0.2 | 27 ± 6 | 0.18 ± 0.01 | 0.17 ± 0.01 | 2.0 ± 0.2 | 1.112 | 2.480 |

[a] [AOT] = 0.10 M; $T$ = 19 ± 1 °C; $W$ = [$H_2O$]/[AOT] and using the constraint $\beta_1 + \beta_2 = 0.35$. The fluorescence lifetimes ($\tau$) correspond to the values of Figure 3. The correlation times, $\phi_1$ and $\phi_2$, are represented in Figure 7. [b] The values of $\phi_{sph}$ were calculated by eq 21. The indicated uncertainties on $\tau$ and $\phi_k$ ($k$ = 1, 2) are 1 standard deviation. The uncertainties on $\phi_{sph}$ were calculated by assuming a relative error of ±15% for the micellar radius.

**Table 4.** Anisotropy Parameters of Cresyl Violet in AOT/Water/*n*-Dodecane Reversed Micelles According to Model 2 (Eq 13) with $\phi_2 = \phi_{sph}$ (Table 3)[a]

| $W$ | $\tau$ (ns) | $\beta_1$ | $\beta_2$ | $\phi_1$ (ns) | $S_p$ | $\theta_p$ (deg) | $(1/\phi_1 - 1/\phi_{sph})^{-1}$ (ns) | $\chi_g^2$ | $Z_{\chi_g^2}$ |
|---|---|---|---|---|---|---|---|---|---|
| 2.7 | 3.04 ± 0.01 | 0.048 ± 0.005 | 0.302 ± 0.005 | 0.36 ± 0.04 | 0.929 ± 0.008 | 18 ± 1 | 0.37 ± 0.04 | 0.982 | −0.382 |
| 5.7 | 2.90 ± 0.02 | 0.095 ± 0.003 | 0.255 ± 0.003 | 2.1 ± 0.1 | 0.854 ± 0.005 | 25.9 ± 0.6 | 2.3 ± 0.1 | 1.115 | 2.486 |
| 10 | 2.81 ± 0.02 | 0.158 ± 0.003 | 0.191 ± 0.003 | 2.7 ± 0.1 | 0.739 ± 0.006 | 35.5 ± 0.5 | 2.9 ± 0.1 | 1.126 | 2.795 |
| 20 | 2.75 ± 0.02 | 0.215 ± 0.002 | 0.135 ± 0.002 | 2.58 ± 0.07 | 0.621 ± 0.005 | 43.8 ± 0.3 | 2.53 ± 0.07 | 1.124 | 2.734 |

[a] [AOT] = 0.10 M; $T$ = 19 ± 1 °C; $W$ = [$H_2O$]/[AOT] and using the constraint $\beta_1 + \beta_2 = 0.35$.

obtained by Beddard et al.[34] We also obtained a value of 0.35 for $\langle r \rangle$ of CV in 1,2−propanediol at −60 °C where rotational motions can be neglected and consequently $\langle r \rangle = r_0$ (see eqs 5 and 10). A similar value was observed in DMSO (unpublished results). These observations attest that $r_0$ is a characteristic of the fluorescence molecule, independent of the solvent in homogeneous solution. The observation that $r_0 = 0.35$ implies that the angle between the absorption and emission dipole moment is not zero.

For CV in water, we obtained $\phi = 0.21 \pm 0.01$ ns at 0.5 °C and $\phi = 0.106 \pm 0.008$ ns at 19 °C with the preexponential factor $\beta$ fixed at 0.35.[34] These $\phi$ values are in good agreement with literature data.[26,33]

In the case of AOT reversed micelles, different expressions for $r(t)$ were used. Each model is discussed separately. Typically, CV and AOT concentrations of $5 \times 10^{-6}$ and 0.1 M, respectively, were used, and the results shown in the figures correspond to those values. The parameters of $r(t)$ do not show a significant dependence on CV concentration.

Unsatisfactory fits were obtained with model 1 for AOT/water/*n*-dodecane reversed micelles. On the other hand, statistically adequate fits were obtained for the system AOT/water/*n*-heptane with global analysis of the decays collected at $\theta = 0°$, 90°, and 54.7°. Values of $\beta$ and the correlation time $\phi$ as a function of $W$ are presented in Figure 5. The recovered values of $\beta$ for the system AOT/water/*n*-heptane are lower than 0.35 (except for $W = 2.7$) and decrease when $W$ is increased (Figure 5a). Therefore, the fact that $\beta$ in model 1 takes up values lower than 0.35 and varies systematically with $W$ in AOT/water/*n*-heptane is taken as an indication that model 1 is not appropriate for AOT reversed micelles (at least for $W \geq 3$). Therefore, model 2 was considered:

model 2

$$f(t) = \alpha \exp(-t/\tau) \tag{13a}$$

$$r(t) = \beta_1 \exp(-t/\phi_1) + \beta_2 \exp(-t/\phi_2) \tag{13b}$$

Statistically adequate fits for both *n*-heptane and *n*-dodecane systems were obtained by using model 2. $Z_{\chi_g^2}$ values were

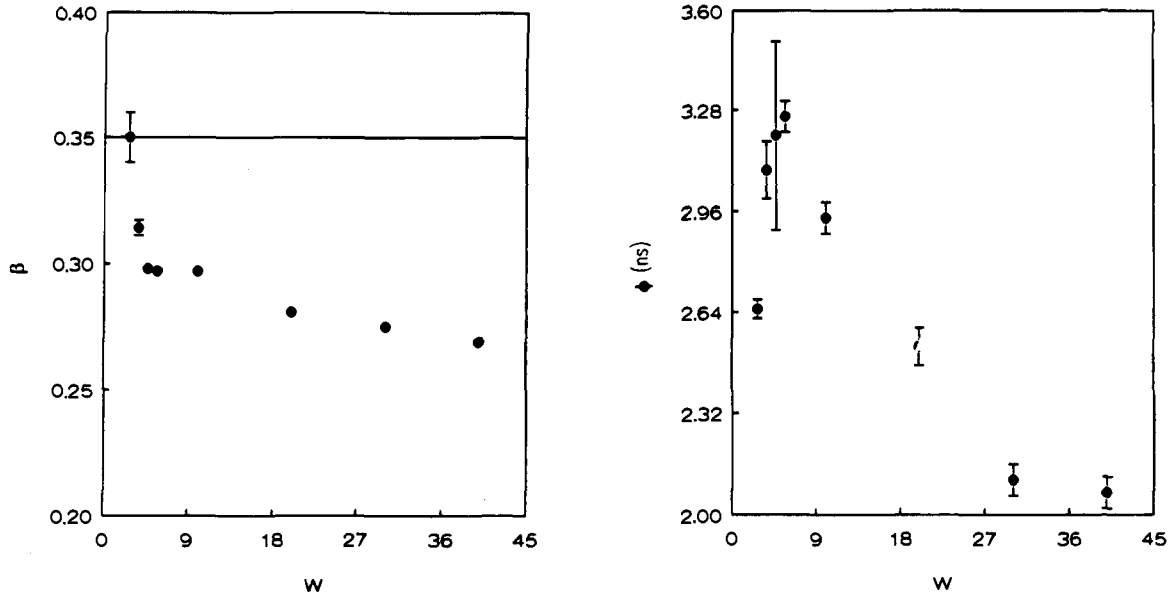


**Figure 5.** 5: Results of model 1 (eq 12) in AOT/water/*n*-heptane: $r(t) = \beta \exp(-t/\phi)$ ($\lambda_{exc}$ = 590 nm). The error bars are 1 standard deviation. (a) $\beta$ vs $W$. The line represents the limiting anisotropy of cresyl violet ($r_0 = 0.35$) when excited in the last absorption band. (b) $\phi$ vs $W$.

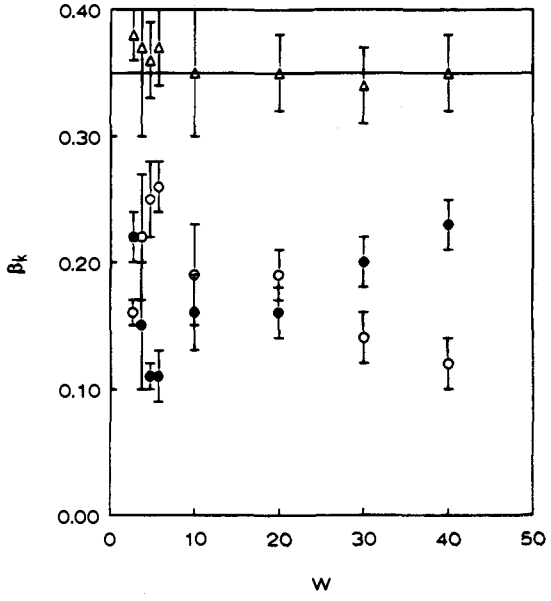


**Figure 6.** 6: $\beta_k$ (as freely adjustable parameters) vs $W$ for model 2 (eq 13) in AOT/water/*n*-heptane: $r(t) = \beta_1 \exp(-t/\phi_1) + \beta_2 \exp(-t/\phi_2)$ with $\phi_1 < \phi_2$. The error bars are 1 standard deviation. (●) $\beta_1$, (○) $\beta_2$, (△) $\beta_1 + \beta_2$, (—) limiting anisotropy 0.35.

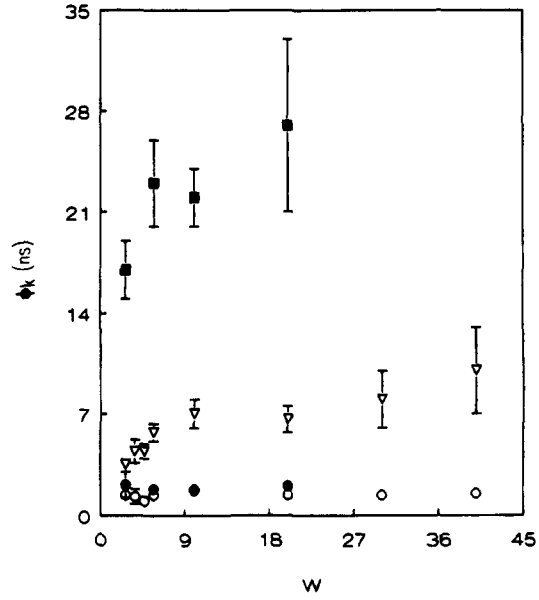


**Figure 7.** 7: $\phi_k$ vs $W$ for model 2 (eq 13), obtained with $\beta_1 + \beta_2 = 0.35$. AOT/water/*n*-heptane: (○) $\phi_1$, (▽) $\phi_2$. AOT/water/*n*-dodecane: (●) $\phi_1$, (■) $\phi_2$. The error bars are 1 standard deviation. The numerical values are shown in Tables 1 and 3.

similar to those recovered for model 1 in the *n*-heptane case. The values obtained for $\tau$ were almost identical to those obtained with model 1. When $\beta_1$ and $\beta_2$ were freely adjustable parameters, the sum $\beta_1 + \beta_2$ for *n*-heptane coincided (within 1 standard deviation) with $r_0 = 0.35$ (Figure 6). When the constraint of $\beta_1 + \beta_2 = 0.35$ was imposed (Tables 1 and 3), the $Z_{\chi_R^2}$ value and the recovered values of $\beta_k$ and $\phi_k$ for the *n*-heptane case were similar to those obtained with $\beta_k$ freely adjustable. The main characteristic of the results obtained by applying model 2 is the dependence of $\beta_k$ on the ratio $W$. This behavior is opposite to the observations in homogeneous solution, where the values of $\phi_k$ but not of $\beta_k$ are affected when the solvent is changed.[26,27]

The shorter correlation time, $\phi_1$, is of similar magnitude (1−2 ns) for both systems and exhibits no systematic dependence on $W$. The longer correlation time, $\phi_2$, is considerably different in the two solvents and increases with $W$ (Figure 7).

For the particular case of the AOT/water/*n*-heptane system at $W = 2.7$, the recovered rotational correlation times were coincident, $\phi_1 = \phi_2 = 2.6$ ns ($\beta_1 + \beta_2$ constrained to 0.35) and with standard deviations on the order of 100%. The same $\phi$ value was recovered using model 1. This could mean that model 1 provides an adequate description of the system at $W = 2.7$ in the AOT/water/*n*-heptane system. However, this is not the case for the *n*-dodecane system, where two well-differentiated rotational correlation times were obtained. For the *n*-heptane system, a value of about 4 ns is expected for $\phi_2$ by extrapolation of the values of the longer rotational correlation time at $W > 2.7$. Hence, the data were analyzed by fixing one rotational correlation time to the average of the $\phi_1$ obtained at the remaining values of $W$ for the same system (1.4 ns), and all other model parameters freely adjustable. In that case a value of $\phi_2 = 3.5 \pm 0.3$ ns was recovered, which approaches the extrapolated value of 4 ns. The recovered preexponential factors were $\beta_1 = 0.10 \pm 0.02$ and $\beta_2 = 0.28 \pm 0.01$. The recovered sum of the preexponential factors was $\beta_1 + \beta_2 = 0.38 \pm 0.02$. Therefore, the apparent coincidence of $\phi_1$ and $\phi_2$ for $W = 2.7$

in the *n*-heptane system seems to be related to difficulties in parameter recovery.

In the case of the AOT/water/*n*-dodecane system the parameters were recovered with high standard deviations when $\beta_1$ and $\beta_2$ were freely adjustable parameters (errors on the order of 100%). When the sum $\beta_1 + \beta_2$ was constrained to 0.35, the standard deviations were substantially reduced. The dependence of $\beta_k$ on $W$ was essentially identical to that for the *n*-heptane system.

Some simulations were performed to investigate the difficulties in the parameter recovery especially for the *n*-dodecane system. Polarized decay curves at $\theta = 0°$, 90°, and 54.7° according to model 2 were simulated ($10^4$ counts at the peak of each decay) using the values of the parameters recovered from the experimental data using model 2 at $W = 10$ in the *n*-heptane and *n*-dodecane systems. The three curves were globally analyzed. When the parameters $\beta_k$ were freely adjustable, the values were recovered with high accuracy and precision for the *n*-heptane system. For the *n*-dodecane system it was necessary to constrain the sum $\beta_1 + \beta_2$ to 0.35 during the analysis to reduce the standard deviation on the parameters (e.g., from 50% to 10% on $\phi_2$). Therefore, the difficulties in recovering the parameters from the experimental decays for the AOT/water/*n*-dodecane system seem not to be related to the quality of the data but rather to the particular combination of parameter values.

An alternative model 3 was considered, based on eq 9 with $L_{jj} = 1$, $L_{jk} = 0$ ($j \neq k$), and $\beta_k = \beta$ ($k = 1,2$):

$$i(\theta,t) = (1/3)\sum_{k=1}^{m}[f_k(t)(1 + (3\cos^2\theta - 1)r_k(t))] \quad (14)$$

where

$$f_k(t) = \alpha_k \exp(-t/\tau_k) \quad (15)$$

$$r_k(t) = \beta \exp(-t/\phi_k) \quad (16)$$

Model 3 corresponds to the case of a heterogeneous ("associative") model where each $\tau_k$ is associated with only one $\phi_k$. Equations 14−16 can describe the case of two groups of dye molecules, each group having its own fluorescence lifetime and rotational correlation time. The use of this model provides an additional check of the number of fluorescence relaxation times of CV in AOT reversed micelles. At each value of $W$ for the AOT/water/*n*-heptane system a global analysis of the three decay curves was performed for freely adjustable $\beta_1$ and $\beta_2$ and for $\beta_1 = \beta_2 = 0.35$. In all cases the values recovered for $\tau_1$ and $\tau_2$ were very similar to the value of $\tau$ shown in Table 1 although the standard deviations were 1 order of magnitude higher. The estimates for $\phi_1$ and $\phi_2$ and their standard deviations were similar if not identical to the values shown in Table 1. In the case of $\beta_1 = \beta_2 = 0.35$ the ratio $\alpha_2/\alpha_1$ decreased monotonically with increasing $W$. Obviously, the change in $\beta_1$ and $\beta_2$ with $W$ in model 2 (Figure 6) is now reflected in $\alpha_1$ and $\alpha_2$. The latter result might suggest that a change in $W$ leads to a change in the relative population of two different sites. However, it is unlikely that two sites would exist in which the dye rotates isotropically with a specific correlation time and which have a similar fluorescence decay time with the same dependence on $W$. Also the global analysis of total intensity decays collected at several emission wavelengths at the same value of $W$, as discussed above, does not support the necessity of these different decay times. Therefore, there is no basis for considering model 3 further in the discussion.

## Discussion

**Spectral Characteristics and Fluorescence Lifetimes.** Cresyl violet perchlorate was found to be insoluble in *n*-heptane and in *n*-dodecane. AOT and CV have opposite charges. The hydrophobic character of the CV aromatic structure limits the solubility in water.[23,24] Therefore, the dye must be localized in the water phase or at the water−surfactant interface. Strong interactions between CV and surfactants forming aqueous micelles have been suggested for cetyltrimethylammonium bromide (CTAB), sodium dodecyl sulfate (SDS), and Triton X-100 aqueous micelles.[24] At the [AOT]/[dye] ratio used in this study, on average no more than one molecule of CV per micelle is present.

In AOT reversed micelles we observed that $\tau$ decreases with increasing $W$. This variation indicates that the average environment of the dye changes with composition. The extent of the decrease of $\tau$ with $W$ is higher for $W \leq 10$ (Figure 3). In that range, the number of water molecules that participate in the hydration of the surfactant polar heads increases from $W = 2$ up to a maximum value at around $W = 10$.[2,51,52] Therefore, the decrease in $\tau$ seems to be correlated with the increase in polar head hydration. This is supported by the observation that the value of $\tau$ at a fixed $W$ is not affected by the organic solvent.

The values of $\tau$ in AOT reversed micelles are systematically higher than in pure water ($\tau = 2.00 \pm 0.02$ ns). The spectral properties of CV in AOT/water/*n*-alkane reversed micelles are different also from the properties in pure water and seem to be more similar to those observed in DMSO.[33]

**Rotational Dynamics According to Model 2.** The values of the rotational correlation times calculated by model 2 at a given value of $W$ can be compared with those obtained in pure water and organic solvents at the same temperature (19−20 °C). In AOT reversed micelles the values of $\phi_1$ and $\phi_2$ are for all $W$ values higher than the correlation time in pure water (0.106 ns) (Tables 1 and 3). This is also reflected by the steady-state anisotropy, which is higher in AOT reversed micelles in comparison with water: $\langle r \rangle \geq 0.16$ in AOT/water/*n*-heptane, $\langle r \rangle \geq 0.20$ in AOT/water/*n*-dodecane, $\langle r \rangle = 0.019$ in pure water. Hence, the rotational properties of CV in AOT reversed micelles are different from those in water, even at high water content ($W = 42$). This is in contrast to the observations with negatively charged perylene derivatives where $\langle r \rangle$ for CV does approach the value obtained in pure water at higher $W$.[47] This is another indication that the dye is mainly located at the surfactant interface, or within the interface, rather than in the water core.

Several researchers[47,51,53,54] have indicated that the time-resolved anisotropy of probes in micelles is a function of two different motions: one is related to the internal restricted rotation of the dye with respect to the micelle (or to the micellar surface); the second one is a slower motion accounting for the rotation of the micelle as a whole. The two motions, "internal" and "slow", are usually and reasonably assumed to be independent,[49,54] in which case the time-resolved anisotropy function $r(t)$ can be expressed as

$$r(t) = \exp(-t/\phi_{mic})\, r_{int}(t) \quad (17)$$

where $r_{int}(t)$ is the internal anisotropy function and $\phi_{mic}$ is the correlation time corresponding to the slower motion.

For the systems under consideration, $r(t)$ is adequately described by a sum of two exponential decays (model 2). Therefore, $r_{int}(t)$ must include two terms. A model of hindered rotation of dye molecules in organized media such as micelles

(51) Wong, W.; Thomas, J. K.; Gratzel, M. *J. Am. Chem. Soc.* **1976**, *98*, 2391.
(52) Politi, M. J.; Brandt, O.; Fendler, J. H. *J. Phys. Chem.* **1985**, *89*, 2345.
(53) Eicke, H.; Zinsli, P. E. *J. Colloid Interface Sci.* **1977**, *65*, 131.
(54) Visser, A. J. W. G.; Vos, K.; van Hoek, A.; Santema, J. S. *J. Phys. Chem.* **1988**, *92*, 759.

may be well approximated as[48,55-59]

$$r_{int}(t) = \beta_1 \exp(-t/\phi_{int}) + \beta_2 \quad (18)$$

where $\phi_{int}$ reflects the motion of the dye inside the micelle. The recovered correlation times $\phi_1$ and $\phi_2$ are expressed as functions of $\phi_{mic}$ and $\phi_{int}$ by combining eqs 17 and 18:

$$\phi_2 = \phi_{mic} \quad (19)$$

and

$$\phi_1 = \left(\frac{1}{\phi_{int}} + \frac{1}{\phi_{mic}}\right)^{-1} \quad (20)$$

This model has been successfully employed for octadecylrhodamine B in AOT reversed micelles (at low values of $W$),[54] for merocyanine 540 and octadecylrhodamine B in aqueous micelles,[60] and for perylene in aqueous micelles.[61] A hindered rotation of CV in AOT reversed micelles can be expected if the dye is attached to the inner micellar surface.

In their study of the fluorescence anisotropy of octadecylrhodamine B in AOT reversed micelles, Visser et al.[54] assumed that $\phi_{mic}$ is equal to the overall rotation correlation time of the micelle being considered as a rigid sphere, $\phi_{sph}$. The estimation of $\phi_{sph}$ at different water contents is not straightforward. If there are no dielectric relaxation effects, then $\phi_{sph}$ will be related to the solution viscosity, $\eta$, by the Debye–Stokes–Einstein model under sticking boundary conditions. Hence,

$$\phi_{sph} = \eta V_h/kT \quad (21)$$

where $\eta$ is the viscosity of the solution, $k$ is Boltzmann's constant, $T$ is the absolute temperature, and $V_h$ is the hydrodynamic volume of the micelle. The viscosity of the solution at 20 °C can be estimated by[62] $\eta = (\eta_{solvent}(1 + [\eta])C)$ where $\eta_{solvent}$ is the viscosity of the pure organic solvent ($\eta_{solvent}$ = 0.417 cP in *n*-heptane, $\eta_{solvent}$ = 1.493 cP in *n*-dodecane),[63] $C$ is the AOT concentration (g/cm$^3$), and $[\eta]$ is the intrinsic viscosity which equals 3.01 cm$^3$/g for [AOT] = 0.10 M in *n*-heptane.[62] At 20 °C the viscosity of the solution is estimated to be 0.471 cP in *n*-heptane. Assuming that $[\eta]$ has the same value in *n*-dodecane, one obtains $\eta$ = 1.687 cP for this solvent.

AOT reversed micelles can be considered as monodisperse to a good approximation,[64] but the hydrodynamic volume is difficult to estimate with sufficient accuracy because its value depends on the radius of the water pool ($r_w$), which includes the polar head, and the surfactant monolayer thickness ($l_c$). $l_c$ is dependent on the solvent, which makes the use of literature values reported for different hydrocarbons difficult. Maitra[38] found that the thickness of the surfactant monolayer in the $H_2O$/AOT/cyclohexane system was around 10 Å. Day et al.[65] estimated the $l_c$ values by the viscometric method and found about 9 Å, although an earlier reported value for the normal length of the AOT molecule was about 11 Å.[66] Approximately the same value was reported by Kotlarchyk et al.[67] in *n*-decane (8 Å) using small-angle neutron scattering. $r_w$ is highly dependent on $W$ but not on the solvent.[64] Using the $r_w$ values in cyclohexane at each value of $W$ as reported by Maitra and assuming $l_c$ = 10 Å (independent of $W$), $V_h$ can be calculated assuming a spherical shape and monodispersity of the micelles. The same values of $r_w$ and $l_c$ were used to calculate $\phi_{sph}$ in *n*-heptane and *n*-dodecane. If the relative error on the total hydrodynamic radius ($r_w + l_c$) is assumed to be ±5%, then the error on $\phi_{sph}$ is approximately ±15% (Tables 1 and 3). The calculated value of $\phi_{sph}$ is in good agreement with the values reported by Visser et al.[54] in *n*-heptane and *n*-decane.

The recovered parameter $\phi_2$ should be equal to $\phi_{mic}$ (eq 19). This seems to be valid for low $W$ values (Tables 1 and 3), and model 2 can be used for the interpretation of the data for $W <$ 10. The correlation time, $\phi_2$, is clearly different from $\phi_{sph}$ (Tables 1 and 3) at higher $W$ values, and the difference increases dramatically with $W$. However, the possibility exists that $\phi_2$ equals $\phi_{sph}$ and that the recovery of this parameter from the experimental data is rather difficult because of the high value of the ratio $\phi_{sph}/\tau$. Therefore, the data were analyzed according to model 2 but with fixing $\phi_2$ to the calculated value of $\phi_{sph}$. The parameters recovered by this analysis are shown in Tables 2 and 4 for the *n*-heptane and *n*-dodecane systems, respectively. Statistically adequate fits were obtained.

The calculated value for the internal rotational motion of the dye, $\phi_{int}$ (eq 20), is reported in Tables 2 and 4. The extent of hindering to $\phi_{int}$ is reflected through the second-order parameter $S_p$:[49,58,75]

$$S_p^2 = \beta_2/r_0 \quad (22)$$

Aspects of the definition and physical interpretation of the order parameter have been widely discussed.[50,58-60,68] The numerical value of $S_p$ ($-1/2 \le S_p \le 1$) is considered as a measure of the spatial restriction of the probe. If $S_p$ = 1, all dye molecules are aligned completely along the axis of the micellar segment, a value of zero is consistent with unrestricted internal rotation, and a value of $-1/2$ corresponds to restriction of the rotation of the probe to a plane perpendicular to the micellar surface.

To get a feeling for the order parameter $S_p$, the data can be interpreted in terms of the wobbling-in-cone model, assuming that the probe has an effective cylindrical symmetry.[50,55,58,60,69] In that model the symmetry axis of the probe diffuses randomly within a cone of semiangle $\theta_p$ measured from the axis perpendicular to the micellar surface. The cone angle $\theta_p$ is related to $S_p$ by

$$S_p = (1/2)\cos\theta_p(1 + \cos\theta_p) \qquad 0° \le \theta_p \le 90° \quad (23)$$

The values of $S_p$ and $\theta_p$ obtained from eqs 22 and 23 are listed in Tables 2 and 4. The value $S_p$ decreases when the water content is increasing. However, it can be expected that a decrease of the order parameter involves an increase of the internal rotational motion of the dye for a constant value of the rotational diffusion constant.[55] This is not observed for the values of $\phi_{int}$ ($\phi_{int} = (1/\phi_1 - 1/\phi_{sph})^{-1}$) reported in Tables 2 and 4 at high $W$. The estimated value of $\phi_{int}$ does not vary substantially with $W$ and is on the order of 2 ns. The semiangle $\theta_p$ ranges from about 20° to 55°, which would suggest a change

(55) Kinosita, K.; Kawato, S.; Ikegami, A. *Biophys. J.* **1977**, *20*, 289.
(56) Dale, R. E.; Chen, L. A.; Brand, L. *J. Biol. Chem.* **1977**, *252*, 7500.
(57) Lakowicz, J. R.; Cherek, H.; Gryczynski, I.; Joshi, N.; Johnson, M. L. *Biophys. J.* **1987**, *51*, 755.
(58) Lipari, G.; Szabo, A. *Biophys. J.* **1980**, *30*, 489.
(59) Wang, S.; Beechem, J. M.; Gratton, E.; Glaser, M. *Biochemistry* **1991**, *30*, 5565.
(60) Quitevis, E. L.; Marcus, A. H.; Fayer, M. D. *J. Phys. Chem.* **1993**, *97*, 5762.
(61) Guang, L.; McGown, L. B. *J. Phys. Chem.* **1993**, *97*, 6745.
(62) Aveyard, R.; Binks, B. P.; Clark, S.; Mead, J. *J. Chem. Soc., Faraday Trans. 1* **1986**, *82*, 125.
(63) Wiswanath, D. S.; Natarajan, G. *Data Book on the Viscosity of Liquids;* Hemisphere Publishing Corp.: Bristol, PA, **1989**.
(64) Almgren, M.; Johannsson, R. *J. Phys. Chem.* **1992**, *96*, 9512.
(65) Day, R. A.; Robinson, B. H.; Clark, J. H. R.; Dokarty, J. V. *J. Chem. Soc.* **1979**, *75*, 132.
(66) Ekwall, P.; Mandell, L.; Fontell, K. *J. Colloid Interface Sci.* **1970**, *33*, 265.
(67) Kotlarchyk, M.; Huang, J. S.; Chen, S. H. *J. Phys. Chem.* **1985**, *89*, 4382.
(68) Heyn, M. *FEBS Lett.* **1979**, *108*, 359.
(69) Ameloot, M.; Hendrickx, H.; Herreman, W.; Pottel, H.; van Cauwelaert, F.; van der Meer, W. *Biophys. J.* **1984**, *46*, 525.

in $\phi_{int}$ by more than a factor of 2.[55] Alternatively, one can assume a change in the rotational diffusion constant such that the order dependence of $\phi_{int}$ is compensated.

The difference between $\phi_2$ and $\phi_{sph}$ in Tables 1 and 3 for $W \geq 10$ can also be explained by other motions of the surfactant besides the overall rotation of the micelle as a rigid sphere. Indeed, even when AOT reversed micelles can be considered to a very good approximation as monodisperse and spherical, they are not "rigid" structures. Motions of one individual surfactant molecule, and of a cluster of surfactant molecules, with respect to the whole micelle are expected on the basis of the dynamic processes reported in reversed micelles.[64] There are two dynamic processes that are expected to have an important influence on the depolarization of dyes in micelles, so that the overall course of depolarization may be more complex than in the simple model above in which $\phi_{mic}$ is identified with $\phi_{sph}$: lateral diffusion of the dye and deformation of the micellar surface.

**(a) Lateral Diffusion of the Dye over the Curved Surface of the Water Pool.** Quitevis et al.[60] have proposed lateral diffusion of merocyanine 540 and octadecylrhodamine B on the surface of aqueous micelles like Triton X-100 or SDS. The chromophores move by exchanging positions or by migrating through interstitial sites.[60] Lateral diffusion of surfactants has been reported in $^{13}C$ spin-relaxation studies of aqueous micelles[70,71] and in microemulsions.[72] In all those studies a correlation time $\phi_L$ given by

$$\phi_L = r^2/4D_L \tag{24}$$

was assigned to the lateral diffusion process, where $r$ is the radius of the spherical surface over which the diffusion occurs and $D_L$ is the lateral diffusion coefficient.

Lateral diffusion of lipids in vesicles above the transition temperature is a well-known process[73,74] with diffusion coefficients on the order of $10^{-8}$ to $10^{-7}$ cm$^2$ s$^{-1}$. In that case, and considering the radius of the lipid vesicles, the values of $\phi_L$ are on the order of microseconds. On the other hand, the lateral diffusion coefficient, $D_L$, of surfactants and chromophores in micelles is expected to be about an order of magnitude higher than in lipid vesicles.[60,70-72,75,76] In general, it has been indicated that the value of $D_L$ should correlate with the value of the packing parameter, $p = v/l_c a_0$ ($a_0$ = area of surfactant polar head, $v$ = volume of surfactant tails, $l_c$ = surfactant monolayer thickness). Translational diffusion coefficients of amphiphilic molecules in the lyotropic liquid crystalline phase have been reported earlier by Lindblom and Wennerström using the pulsed NMR magnetic field gradient method.[75] These and other researchers[60,70-72] have reported values of $D_L$ on the order of $10^{-6}$ cm$^2$ s$^{-1}$ for surfactants and chromophores in aqueous micelles. Considering that the radii of aqueous micelles are on the order of $10^{-7}$ cm, and $D_L \approx 10^{-6}$ cm$^2$ s$^{-1}$, values of $\phi_L \approx 10^{-9}$ s are predicted. Therefore, lateral diffusion may, in principle, make a significant contribution to fluorescence depolarization in aqueous micelles, as has been pointed out by Grieser and Drummond.[76] The same is expected for reversed micelles,[72] although no indication of this possibility seems to have appeared so far in the literature concerning fluorescence depolarization in reversed micelles.

If the difference between $\phi_2$ and $\phi_{sph}$ is due to lateral diffusion, the relevant correlation time, $\phi_L$, is given by $1/\phi_L = 1/\phi_2 - 1/\phi_{sph}$. The values of $\phi_L$ thus obtained are significantly different in *n*-heptane and *n*-dodecane: $\phi_L$(heptane) < $\phi_L$(dodecane). While this would be consistent with the relative viscosities, $\phi_L$ in each solvent is not influenced by $W$, i.e., does not appear to depend on the size of the micelle. This observation attests that lateral diffusion has little influence on the depolarization process. In fact, the rate of lateral diffusion is expected to be strongly dependent on the micellar packing, which is in turn highly dependent on $W$.[38] Besides, according to hydrodynamic models for lateral diffusion such as those used in studies of lipid vesicles,[73] the viscosity of the organic solvent is not expected to have a drastic influence on the lateral diffusion of the chromophore over the water pool surface. To evaluate this observation for the current systems, $D_L$ was calculated from $\phi_L$ obtained using eq 24. The values range from a plateau value at about $0.3 \times 10^{-6}$ cm$^2$ s$^{-1}$ for $W \leq 6$ for the *n*-heptane system and increase monotonically to a value of $8 \times 10^{-6}$ cm$^2$ s$^{-1}$ at $W = 40$, with no indication of a plateau at high water content. This dependence of the calculated $D_L$ is completely at variance with the expected dependence of the packing parameter on $W$ discussed above.

**(b) Deformation of the Micellar Surface ("Breathing") Due to a Cooperative Motion of a Group of Surfactant Molecules.** At the relatively low micelle concentrations used in this work ([micelle] $\cong 10^{-4}$ M) the exchange between micelles during collisions is a slow process whose contribution to the depolarization must be negligible. However, micelles deform rather easily as has been described by Walderhaug et al.[70] These researchers indicated that deformation of the micelle shape would contribute to the spin-relaxation (NMR depolarization). In contrast to $\phi_L$, the correlation time associated with the breathing, $\phi_b$, is expected to be influenced by the viscosity or density of the organic solvent. With respect to the micelle as a whole this motion would have a restricted angular amplitude. A schematic representation of the model including the breathing of the micelle is given in Figure 8.

The possibility that the difference between $\phi_{mic}$ and $\phi_{sph}$ at $W \geq 10$ could be explained by a deformation of the micellar surface necessitates the use of a more elaborated model. Indeed, the contribution to the anisotropy decay by the deformation cannot be described by a single exponential. Such a simple decay would imply that the director associated with the group of molecules involved in the deformation describes an isotropic rotation. In the elaborate model it will be assumed again that the motions of the total micelle and of the surfactant molecules involved in the deformation are uncoupled. Under this assumption the total anisotropy decay, to be referred to as model 4, can be written as

$$r(t) = r_p(t)\, r_b(t) \exp(-t/\phi_{sph}) \tag{25}$$

$r_p(t)$ reflects the local motion of the probe and can be expressed as

$$r_p(t) = \beta_{p1} \exp(-t/\phi_p) + \beta_{p2} \tag{26}$$

with

$$\beta_{p1} + \beta_{p2} = r_0 \tag{27}$$

$r_b(t)$ is associated with the breathing motion and can be written as

(70) Walderhaugh, H.; Söderman, O.; Stilbs, P. *J. Phys. Chem.* **1984**, *88*, 1655.
(71) Néry, H.; Söderman, O.; Canet, D.; Walderhaug, H.; Lindman, B. *J. Phys. Chem.* **1986**, *90*, 5802.
(72) Ahlnäs, T.; Söderman, O.; Hjelm, C.; Lindman, B. *J. Phys. Chem.* **1983**, *87*, 822.
(73) Silver, B. L. *The Physical Chemistry of Membranes*; Solomom Press: New York, 1985; Chapter 10, p 231.
(74) Edidin, M. Rotational and Translational Diffusion in Membranes. *Annual Review of Biophysics and Bioengineering*; Mullis, L. J., Hagins, W. A., Stryer, L., Newton, C., Eds.; Annual Reviews, Inc.: Palo Alto, CA, 1974; Vol. 3, p 179.
(75) Lindblom, G.; Wennerström, H. *Biophys. Chem.* **1977**, *6*, 167.
(76) Grieser, F.; Drummond, C. J. *J. Phys. Chem.* **1988**, *92*, 5580.

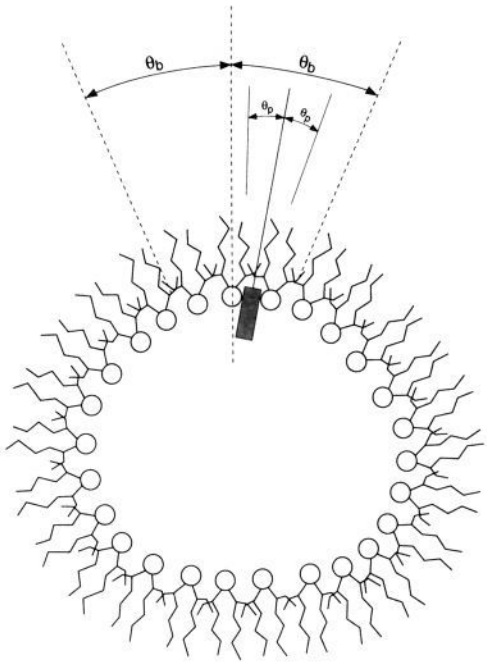


**Figure 8.** 8: Schematic representation of model 4 (eq 25) including the breathing of the micelle. $\theta_p$ and $\theta_b$ describe the extent of the motion of the probe and the micellar segment, respectively.

$$r_b(t) = \beta_{b1} \exp(-t/\phi_b) + \beta_{b2} \tag{28}$$

with

$$\beta_{b1} + \beta_{b2} = 1 \tag{29}$$

$\beta_{b2}$ is a measure of the extent of the breathing. Small values of $\beta_{b2}$ correspond to large deformations. $\phi_b$ is a measure of the rate of the motion of the micellar segment.

Under the approximation that

$$\frac{1}{\phi_p} + \frac{1}{\phi_b} \cong \frac{1}{\phi_p} \tag{30}$$

the overall anisotropy decay $r(t)$ is a triple exponential

$$r(t) = \sum_{j=1}^{3} \beta_j \exp(-t/\phi_j) \tag{31}$$

where

$$\beta_1 = \beta_{p1} \tag{32a}$$

$$\beta_2 = \beta_{p2}\beta_{b1} \tag{32b}$$

$$\beta_3 = \beta_{p2}(1 - \beta_{b1}) \tag{32c}$$

and

$$\phi_1 = \left(\frac{1}{\phi_p} + \frac{1}{\phi_{sph}}\right)^{-1} \tag{33a}$$

$$\phi_2 = \left(\frac{1}{\phi_b} + \frac{1}{\phi_{sph}}\right)^{-1} \tag{33b}$$

$$\phi_3 = \phi_{sph} \tag{33c}$$

It is clear that

$$\beta_1 + \beta_2 + \beta_3 = r_0 \tag{34}$$

$$\beta_{b2} = \frac{\beta_3}{\beta_2 + \beta_3} \tag{35}$$

The extent of the hindering to the internal rotational motion of the dye is reflected through the second-order parameter $S_p$:[49,58,75]

$$S_p^2 = \frac{\beta_{p2}}{r_0} = \frac{\beta_2 + \beta_3}{r_0} \tag{36}$$

Similarly, the extent of the hindering to the motion of the micellar segment is expressed by the second-order parameter $S_b$:

$$S_b^2 = \beta_{b2} \tag{37}$$

The data were analyzed according to model 4 with the sum of $\beta_j$ constrained to 0.35 and $\phi_3$ fixed to the calculated value of $\phi_{sph}$ shown in Tables 1 and 3. The decays collected for $\theta$ = 0°, 54.7°, and 90° were globally analyzed for each $W$, in the same way as was described for model 2. The parameters recovered by this analysis are shown in Tables 5 and 7 for the *n*-heptane and *n*-dodecane systems, respectively. For $W = 5.7$ physically unacceptable parameters were obtained for *n*-heptane (Table 5) and parameters with large errors for *n*-dodecane (Table 7). This suggests that model 4 is not applicable at this intermediate $W$-value. From Tables 5 and 7, one can see that the assumption expressed by eq 30 is confirmed and that the correlation time $\phi_1$ is short enough in comparison with $\phi_{sph}$ not to be affected significantly by the overall rotation of the micelle so that, to a very good approximation (see eq 33a)

$$\phi_1 = \phi_p \tag{38}$$

The rotational correlation time associated with the breathing, $\phi_b$, was calculated from eq 33b, for $W \geq 10$. The recovered values of $\phi_b$ for each value of $W$ seem to be higher in *n*-dodecane than in *n*-heptane (Tables 6 and 8). The parameter $S_b$ reflects the extent of the restriction for the breathing: $S_b \cong 0.4$ in *n*-heptane, $S_b \cong 0.7$ in *n*-dodecane. Both parameters, $\phi_b$ and $S_b$, are higher in *n*-dodecane than in *n*-heptane as expected from the relative viscosities.

The values of $S_p$ obtained from eq 36 are listed in Tables 6 and 8. The values of $S_p$ are around 0.9, indicating that the internal rotation of the dye with respect to the micelle is highly restricted. In other words, the contribution of the probe to the depolarization in model 2 is now mainly accounted for by the motion of the micellar segment.

Within the wobbling-in-cone model, the symmetry axis of the probe diffuses randomly within a cone of semiangle $\theta_p$ measured from the axis of the embedding micellar segment (Figure 8). An analogous reasoning can be followed for $\theta_b$, where $\theta_b$ is defined with respect to the normal to the micellar surface (Figure 8). The values of $\theta_p$ and $\theta_b$ are reported in Tables 6 and 8. Comparing *n*-heptane and *n*-dodecane, it is important to notice that $\theta_b$ is smaller in *n*-dodecane, the solvent with the higher bulk viscosity.

## Conclusion

The time-resolved fluorescence anisotropy decay $r(t)$ of CV in AOT/water/*n*-heptane and AOT/water/*n*-dodecane can be described with a sum of two exponential functions. For $W <$ 10 the parameter values in this biexponential description can be interpreted in terms of a physical model (model 2). The longest rotational correlation time matches the value expected for the overall rotation of the micelle. The shortest rotational correlation time describes the wobbling motion of the probe within a restricted environment. An association between the

**Table 5.** Anisotropy Parameters of Cresyl Violet in AOT/Water/*n*-Heptane Reversed Micelles According to Model 4 (Eq 25)[a]

| $W$ | $\phi_1$ (ns) | $\phi_2$ (ns) | $\beta_1$ | $\beta_2$ | $\beta_3$ | $\chi_g^2$ | $Z_{\chi_g^2}$ |
|---|---|---|---|---|---|---|---|
| 5.7 | 1.4 ± 0.6 | 8 ± 32 | 0.11 ± 0.09 | −0.49 ± 27 | 0.73 ± 27 | 0.992 | −0.223 |
| 10 | 0.4 ± 0.1 | 3.0 ± 0.2 | 0.04 ± 0.01 | 0.268 ± 0.009 | 0.04 ± 0.04 | 1.069 | 1.821 |
| 20 | 0.6 ± 0.2 | 3.0 ± 0.3 | 0.06 ± 0.02 | 0.25 ± 0.01 | 0.04 ± 0.02 | 1.067 | 1.751 |
| 30 | 0.7 ± 0.2 | 2.8 ± 0.4 | 0.08 ± 0.03 | 0.23 ± 0.03 | 0.04 ± 0.03 | 1.064 | 1.679 |
| 40 | 0.5 ± 0.2 | 2.4 ± 0.2 | 0.05 ± 0.02 | 0.25 ± 0.02 | 0.05 ± 0.03 | 1.095 | 2.538 |

[a] [AOT] = 0.10 M; $T$ = 19 ± 1 °C; $W$ = [$H_2O$]/[AOT] and using the constraint $\beta_1 + \beta_2 + \beta_3 = 0.35$. For each $W$, the correlation time $\phi_3$ was fixed to $\phi_{sph}$ (values shown in Table 1). The uncertainties are 1 standard deviation.

**Table 6.** Order and Wobbling-in-Cone Parameters of Cresyl Violet in AOT/Water/*n*-Heptane Reversed Micelles Corresponding with Model 4 (Eq 25)

| $W$ | $\beta_{b2}$ | $\phi_b$ (ns) | $S_p$ | $\theta_p$ (deg) | $S_b$ | $\theta_b$ (deg) |
|---|---|---|---|---|---|---|
| 10 | 0.13 ± 0.04 | 3.8 ± 0.3 | 0.94 ± 0.02 | 16 ± 3 | 0.36 ± 0.05 | 61 ± 3 |
| 20 | 0.14 ± 0.07 | 3.2 ± 0.3 | 0.91 ± 0.03 | 20 ± 4 | 0.37 ± 0.09 | 60 ± 6 |
| 30 | 0.15 ± 0.07 | 2.9 ± 0.4 | 0.88 ± 0.05 | 23 ± 5 | 0.39 ± 0.09 | 59 ± 6 |
| 40 | 0.17 ± 0.08 | 2.4 ± 0.2 | 0.93 ± 0.02 | 18 ± 5 | 0.4 ± 0.1 | 58 ± 7 |

**Table 7.** Anisotropy Parameters of Cresyl Violet in AOT/Water/*n*-Dodecane Reversed Micelles According to Model 4 (Eq 25)[a]

| $W$ | $\phi_1$ (ns) | $\phi_2$ (ns) | $\beta_1$ | $\beta_2$ | $\beta_3$ | $\chi_g^2$ | $Z_{\chi_g^2}$ |
|---|---|---|---|---|---|---|---|
| 5.7 | 0.7 ± 0.7 | 3 ± 1 | 0.03 ± 0.03 | 0.08 ± 0.03 | 0.24 ± 1 | 1.113 | 2.453 |
| 10 | 1.3 ± 0.5 | 7 ± 5 | 0.08 ± 0.04 | 0.12 ± 0.02 | 0.15 ± 0.09 | 1.108 | 2.403 |
| 20 | 1.3 ± 0.7 | 4 ± 2 | 0.09 ± 0.08 | 0.15 ± 0.07 | 0.11 ± 0.10 | 1.113 | 2.491 |

[a] [AOT] = 0.10 M; $T$ = 19 ± 1 °C; $W$ = [$H_2O$]/[AOT] and using the constraint $\beta_1 + \beta_2 + \beta_3 = 0.35$. For each $W$, the correlation time $\phi_3$ was fixed to $\phi_{sph}$ (values shown in Table 3). The uncertainties are 1 standard deviation.

**Table 8.** Order and Wobbling-in-Cone Parameters of Cresyl Violet in AOT/Water/*n*-Dodecane Reversed Micelles Corresponding with Model 4 (Eq 25)

| $W$ | $\beta_{b2}$ | $\phi_b$ (ns) | $S_p$ | $\theta_p$ (deg) | $S_b$ | $\theta_b$ (deg) |
|---|---|---|---|---|---|---|
| 10 | 0.55 ± 0.09 | 8 ± 7 | 0.88 ± 0.06 | 23 ± 7 | 0.74 ± 0.06 | 35 ± 6 |
| 20 | 0.4 ± 0.3 | 4 ± 2 | 0.86 ± 0.10 | 25 ± 11 | 0.7 ± 0.2 | 38 ± 16 |

probe CV and the AOT molecules can be expected because of their opposite charges. This picture is supported by the value of the fluorescent lifetimes at the various water concentrations. For $W \geq 10$ the interpretation is not straightforward because the longest rotational correlation time differs significantly from the expected rotational correlation time of the micelle. One of the possibilities is that the rotation of the micelle cannot be recovered accurately because of the relatively short fluorescence lifetime of the probe. Statistically acceptable fits can be obtained with the biexponential description in which the longest rotational correlation time is kept fixed to the predicted value for the rotational motion of the micelle. However, the corresponding values for rate and the extent of the wobbling motion probe at the higher water concentrations appear to be not entirely consistent. Therefore, for $W \geq 10$ a more elaborate model (model 4) is suggested which includes the motion of micellar segments with respect to the overall micellar structure. This so-called breathing motion has been suggested in the literature, but no quantification had been reported so far. The alternative model 4 for $r(t)$ includes the depolarization due to (a) the local motion of the probe within its restricted environment ($r_p(t)$), (b) the motion of the micellar segment containing the dye ($r_b(t)$), and (c) the overall rotation of the micelle. Both $r_p(t)$ and $r_b(t)$ were expressed as the sum of an exponential decay and a constant. The constant value in $r_p(t)$ gives an indication of the width of the distribution of the dye within the micellar segment; i.e., the constant is correlated with the second orientational order parameter $S_p$. Similarly, the limiting value in the expression for $r_b(t)$ measures the second-order parameter $S_b$ of the equilibrium distribution of the micellar segments with respect to the normal to the micellar surface. In the data analysis a triple exponential approximation to model 4 was used. It was found that $S_p$ was about 0.9 at high $W$ values. The value of $S_p$ did not depend on the continuous phase. The high value of $S_p$ is consistent with the model in which CV is not located in the water core but is embedded within the interface region. Because of the high value of $S_p$, one can expect that the dye molecule moves together with a number of neighboring surfactant molecules. $S_b$ was higher in *n*-dodecane than in *n*-heptane. The relaxation time $\phi_b$ in $r_b(t)$ measures the dynamics of the wobbling motion of the micellar segment and was found to be on the order of several nanoseconds. As expected, $\phi_b$ is higher in *n*-dodecane than in *n*-heptane. The rather small values for $S_b$ and $\phi_b$ reflect the generally accepted dynamic nature of the micelle.

At this point, no definite choice between model 2 or model 4 at higher water content can be made. The parameters obtained within model 4 represent an internally consistent model whose validity should be checked with other dyes.

**Acknowledgment.** N.W. thanks the IWONL for a predoctoral fellowship. R.M.N. thanks the Fundación Antorchas (Argentina) for financial support and KUL for a postdoctoral fellowship. The continuing support of the FKFO and the Ministry of "Wetenschapsbeleid" through Grants IUAP-II-16 and IUAP-III-040 is gratefully acknowledged. N. Boens is thanked for the implementation and development of the software used in the analysis of the fluorescence decays. The authors gratefully acknowledge the stimulating discussions with R. E. Dale.